JACS
JOURNAL OF THE AMERICAN CHEMICAL SOCIETY
Article
pubs.acs.org/JACS

DFT Computational Study of the Methanolytic Cleavage of DNA and RNA Phosphodiester Models Promoted by the Dinuclear $Zn^{(II)}$ Complex of 1,3-Bis(1,5,9-triazacyclododec-1-yl)propane

Christopher I. Maxwell,*[,†] Nicholas J. Mosey,*[,‡] and R. Stan Brown*[,‡]

[†]Uppsala Biomedicinska Centrum, BMC, Husarg. 3, Box 596, 751 24 Uppsala, Sweden
[‡]Department of Chemistry, Queen's University, Kingston, Ontario, Canada K7L 3N6

Supporting Information

ABSTRACT: A density functional theory study of the cleavage of a DNA model [*p*-nitrophenyl methyl phosphate (**2**)] and two RNA models [*p*-nitrophenyl 2-hydroxypropyl phosphate (**3**) and phenyl 2-hydroxypropyl phosphate (**4**)] promoted by the dinuclear $Zn^{(II)}$ complex of 1,3-bis(1,5,9-triazacyclododec-1-yl)propane formulated with a bridging methoxide (**1a**) was undertaken to determine possible mechanisms for the transesterification processes that are consistent with experimental data. The initial substrate-bound state of **2**:**1a** or **3**:**1a** has the two phosphoryl oxygens bridging $Zn^{(II)}_1$ and $Zn^{(II)}_2$. For each of **2** and **3**, four possible mechanisms were investigated, three of which were consistent with the overall free energy for the catalytic cleavage step for each substrate. The computations revealed various roles for the metal ions in the three mechanisms. These encompass concerted or stepwise processes, where the two metal ions with associated alkoxy groups [$Zn^{(II)}_1$:($^-OCH_3$) and $Zn^{(II)}_1$:($^-$O-propyl)] play the role of a direct nucleophile (on **2** and **3**, respectively) or where $Zn^{(II)}_1$:($^-OCH_3$) can act as a general base to deprotonate an attacking solvent molecule in the case of **2** or the attacking 2-hydroxypropyl group in the case of **3**. The $Zn^{(II)}_2$ ion can serve as a spectator (after exerting a Lewis acid role in binding one of the phosphates' oxygens) or play active additional roles in providing direct coordination of the departing aryloxy group or positioning a hydrogen-bonding solvent to assist the departure of the leaving group. An important finding revealed by the calculations is the flexibility of the ligand system that allows the Zn−Zn distance to expand from ∼3.6 Å in **1a** to over 5 Å in the transforming **2**:**1a** and **3**:**1a** complexes during the catalytic event.

INTRODUCTION

Considerable effort has been expended to develop dinuclear metal-containing complexes as models for metallonucleases that are capable of promoting the solvolytic cleavage of phosphodiesters.[1−5] The overall processes for those reactions involving substrates modeling the phosphodiester linkage in DNA with $(RO)(ArO)PO_2^-$ can be represented as in eqs 1 and 2 (using a shorthand representation for a dinuclear $Zn^{(II)}$ catalyst with a bridging lyoxide). Possible mechanisms for the cleavage of DNA models can involve direct nucleophilic attack of a metal-coordinated lyoxide on the phosphorus with concerted displacement of the leaving group or the formation of a five-coordinate phosphorane intermediate that subsequently breaks down to give products. In the case of 2-hydroxypropyl-containing substrates that model the phosphodiester in RNA, $(HOCH(CH_3)CH_2O)(ArO)PO_2^-$, the cyclization reaction shown in eq 2 involves intramolecular closure of the 2-propoxy group on the phosphorus with concerted or stepwise cleavage of the leaving group. There is considerable debate in the literature whether the catalyzed reactions in eq 2 are concerted or stepwise and whether the deprotonation of the 2-propoxy group occurs with general base catalysis provided by the internal $Zn^{(II)}$-coordinated lyoxide concurrent with nucleophilic attack on P or by specific base catalysis with a pre-equilibrium formation of the 2-propoxy anion prior to nucleophilic attack on P. Evidence for both possibilities exists, although it comes from different dinuclear $Zn^{(II)}$-containing catalysts in different solvent mixtures, namely, water[4] and the light alcohols methanol and ethanol.[2]

Earlier we presented[2] extensive kinetic data for the methanolytic cleavage of two series of phosphate diesters related to the DNA- and RNA-type models in eqs 1 and 2 promoted by the dinuclear $Zn^{(II)}$ complex of 1,3-bis(1,5,9-triazacyclododec-1-yl)propane formulated with a bridging

Received: August 26, 2013
Published: October 10, 2013

   dx.doi.org/10.1021/ja4088264 | J. Am. Chem. Soc. 2013, 135, 17209−17222

methoxide (**1a**). On the basis of work with DNA models such as **2** and RNA models such as **3** and **4**, the experimental results suggested the general mechanism shown in eq 3, where **Lig**

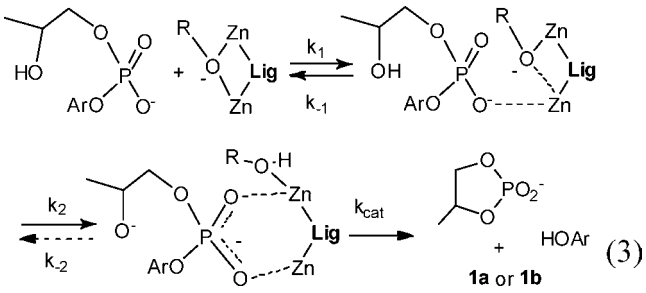

(3)

refers to the 1,3-bis(1,5,9-triazacyclododec-1-yl)propane ligand. The precatalytic form of the catalyst is believed to have a bridging alkoxide, and the two $Zn^{(II)}$ ions bind to the substrate in a two-step process[2a,c] involving first one phosphoryl nonbridging oxygen and then the second. With fast-reacting substrates having a good leaving group (LG) such as *p*-nitrophenoxy, the second step (k_2), possibly one of binding to the second $Zn^{(II)}$, is rate-limiting, and the subsequent chemical cleavage steps are fast. For slower-reacting substrates, there is complete equilibrium binding of the substrate followed by a series of chemical steps.[2a] In the case of the cleavage of 2-hydroxypropyl aryl phosphates **3** and **4**, the intramolecular cyclization process depicted in eq 2 was suggested to involve a general-base-promoted abstraction of the 2-propoxy hydrogen by $Zn^{(II)}$–$^{-}$OR because the cleavage rates observed in ethanol exceeded the diffusion-limited rate constant for proton abstraction by external ethoxide base in a specific-base process.[2g] The overall nucleophilic cleavage of the aryloxy group in **3** and **4** mediated by **1a** was considered to be consistent with either a stepwise or concerted process.[2a] For **1a**-catalyzed cleavage of the slower-reacting DNA substrates such as **2**, the mechanism appears to involve pre-equilibrium binding of the substrate with each of the two nonbridging phosphoryl oxygens ligated to a different $Zn^{(II)}$, followed by intramolecular cleavage of the aryloxy group by a concerted or stepwise process. Since the Brønsted plots that were observed with cleavage of DNA models were linear, if the cleavage was stepwise, the rate-limiting step was nucleophilic attack.

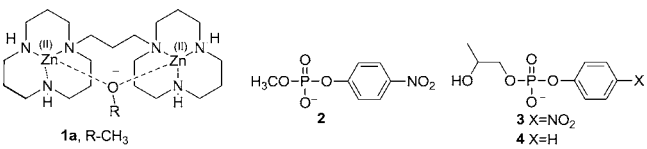

There are mechanistic questions that cannot be answered with certainty from the experimental studies, so what concerns us here is a density functional theory (DFT) computational study of the cleavage of **2**, **3**, and **4** promoted by **1a**. Similar computational studies have recently been reported by two groups[6,7] for the cyclization of **3** promoted by dinuclear complex **5**, the mechanism of which has been delineated in several key experimental studies by Richard, Morrow, and co-workers.[4a–g,j,k] The proposed mechanisms based on the two studies were different in terms of specific base and concerted reaction[6] versus general base and stepwise reaction,[7] although the findings of the former DFT study were more consistent with the experimental evidence.[4] In light of these two reports, the study of the details of the **1a**-promoted cleavages of **2**–**4** is warranted because this ligand system is far more flexible than **5** and at the same time is more active in terms of rate for the cleavage of phosphodiesters.[2a,c–f,i–m] Such flexibility may influence the catalytic prowess greatly, since **6** with its fixed bridging 2-oxo group is 37 000 times less active than **1a** in promoting the cyclization of **3** in methanol.[2b] Furthermore, both **1a** and **1b** have the ability to cleave RNA models as well as far less reactive DNA models, and their catalyzed reactions in methanol and ethanol are faster by several orders of magnitude[8,9] than any reported to date in aqueous media.[3–5]

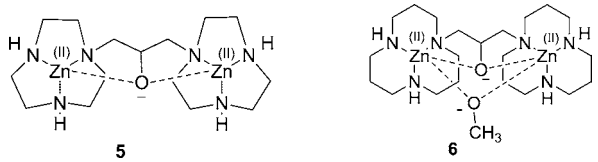

COMPUTATIONAL DETAILS

Geometries were optimized using density functional theory (DFT) with the B3LYP[10] functional. The 6-31G(d,p) basis set was used for carbon and hydrogen atoms, while diffuse functions were added for oxygen, nitrogen, and phosphorus [6-31++G(d,p)]. Hay and Wadt's effective core potential with the double-ζ valence basis set (LANL2DZ[11]) was used to describe zinc. Frequency calculations were conducted as a basis for free energy calculations and to characterize structures as intermediates or transition states. The IEFPCM[12] solvation model was employed in all of the calculations, so the energy values reported refer to solution values at this level of theory. All of the calculations were completed using the Gaussian 09 program.[13] The computational methodology used here is at a similar level to that used successfully and tested against several alternative levels of theory by Gao and co-workers[6] for their study involving the cleavage of **3a** promoted by catalyst **5**.

For the cleavage of each of **2** and **3**, four possible mechanisms were tested. Some of the mechanisms involved the addition and direct participation of methanol molecules from the surrounding bulk solvent environment. To maintain atom balance throughout the calculations, the energetic contributions of a solvated methanol molecule must be accurately represented, but this poses two challenges. First, a solvated methanol is stabilized by the hydrogen-bonding network of the bulk solvent, and we accounted for this effect here and previously[14] by representing the energy contributions of methanol with a fractional value of an IEFPCM-solvated methanol hexamer. The second challenge involves accurately representing the entropy associated with the bimolecular process of adding or removing a methanol molecule. The estimation of the free energies associated with bimolecular processes such as these tends to be inaccurate as a result of overestimation of the entropic contributions of rotational and translational movements because a solvated molecule's translational and rotational motion is highly (although not entirely) suppressed by the bulk solvent. In order to obtain free energy calculations closer to those experimentally observed, we employed the method used by Sakaki and co-workers[15] and calculated a corrected free energy without entropic contributions due to translation and rotation (cf. eqs 4 and 5). While this admittedly underestimates the true ΔG, there are convincing arguments[15] that ΔG_{corr} is more accurate when describing bimolecular processes occurring in solvent.

$$\Delta G = \Delta H - T(\Delta S_{elec} + \Delta S_{trans} + \Delta S_{rot} + \Delta S_{vib}) \quad (4)$$

$$\Delta G_{corr} = \Delta H - T(\Delta S_{elec} + \Delta S_{vib}) \quad (5)$$

RESULTS

a. Substrate Binding. The starting point for the initial structure optimization for **1a** was constructed with careful

dx.doi.org/10.1021/ja4088264 | J. Am. Chem. Soc. 2013, 135, 17209–17222

examination of a previously published X-ray diffraction structure of the corresponding bridged hydroxo complex.[2a] The structure is such that the ligand N−H groups on the two 1,5,9-triazacyclododecane units are oriented into the active cleft of the complex. In the optimized structure, shown in Figure 1,

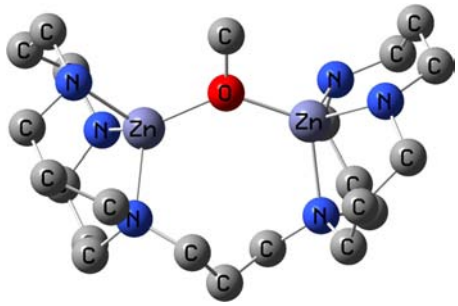

Figure 1. DFT-optimized structure of **1a**.

the methoxide moiety bridges the tetrahedral $Zn^{(II)}$ ions, with the 1,3-bis(1,5,9-triazacyclododec-1-yl)propane ligand encompassing the metal ions in an earmufflike motif. Here the metal ions are held in close proximity (3.709 Å apart) and are conjoined by a bridging methoxide that rigidifies the complex, holding the two metal ions in close enough proximity that they act cooperatively in substrate binding and in the subsequent steps for catalyzing the cleavage of the phosphate diesters (vide infra). The substrate binding process for the DNA model (**2** + **1a** → **2**:**1a**) is exergonic with ΔG_{corr} = −23.4 kcal mol^{-1}, a computed value that is unlikely to be close to the real value as these calculations do not involve explicit solvent−solute interactions that stabilize the +3 charge of the dinuclear $Zn^{(II)}$ complex or the monoanionic phosphate diester **2**. The substrate coordination modes in **2**:**1a** (Figure 2, structure SM_2) and the 2-hydroxypropyl *p*-nitrophenyl phosphate derivative **3**:**1a** were modeled after that for binding of dibenzyl phosphate to the reported X-ray diffraction structure of the corresponding dinuclear $Cu^{(II)}$ complex[2c] under the assumption that the binding modes should be similar. Here the substrate is coordinated to both $Zn^{(II)}$ ions, each of which has trigonal-bipyramidal coordination with a different phosphate oxygen occupying an axial position. The inter-$Zn^{(II)}$ distance expands by 0.09 Å to 3.799 Å upon substrate binding.

b. Mechanisms for Chemical Steps for the Methanolysis of 2 Catalyzed by 1a. A variety of potential mechanisms involving various steps shown in Schemes 1 and 2

Scheme 1. Initial Dissociation of the Bridging Methoxide Moiety from $Zn^{(II)}_2$ (Relative Free Energies Are Reported in kcal mol^{-1})

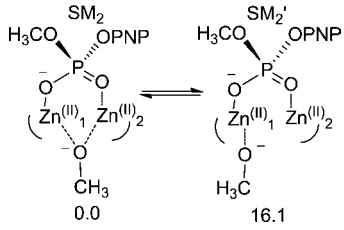

were envisioned to be possible during the **1a**-catalyzed methanolysis of DNA model **2**. The mechanisms, shown in more detail in Scheme 2, often involve several slightly rearranged intermediates of similar energies along the reaction coordinate, so only those intermediates that are deemed mechanistically relevant are shown.

Given the premise that a doubly $Zn^{(II)}$-coordinated methoxide is unlikely to be sufficiently nucleophilic to attack a coordinated phosphate diester,[2] each of these mechanisms requires a preliminary step in which one of the $Zn^{(II)}$−($^{-}OCH_3$) bonds in **2**:**1a** breaks to give the open form SM_2', in which the methoxide remains ligated to a single $Zn^{(II)}$, denoted as $Zn^{(II)}_1$:($^{-}OCH_3$). This loosens the inter-$Zn^{(II)}$ distance, with the tetracoordinated $Zn^{(II)}_2$ ion becoming tetrahedral and more exposed on the reverse side of the structure, as represented by the transition from SM_2 to SM_2' in Figure 2. While a distinct transition state for this process could not be found, potential energy surface scans indicated that the barrier is similar to that of the SM_2' structure, roughly 16.1 kcal mol^{-1} above SM_2.

Four mechanisms, given in Schemes 2−5 and discussed below, are accessible from the SM_2' structure through the addition of methanol molecules, either donating a hydrogen bond to the methoxide or coordinating with the tetrahedral $Zn^{(II)}_2$. Presented along with the mechanisms are the corresponding free energies (in kcal mol^{-1} relative to the SM_2 structure) of the intermediates and transition states.

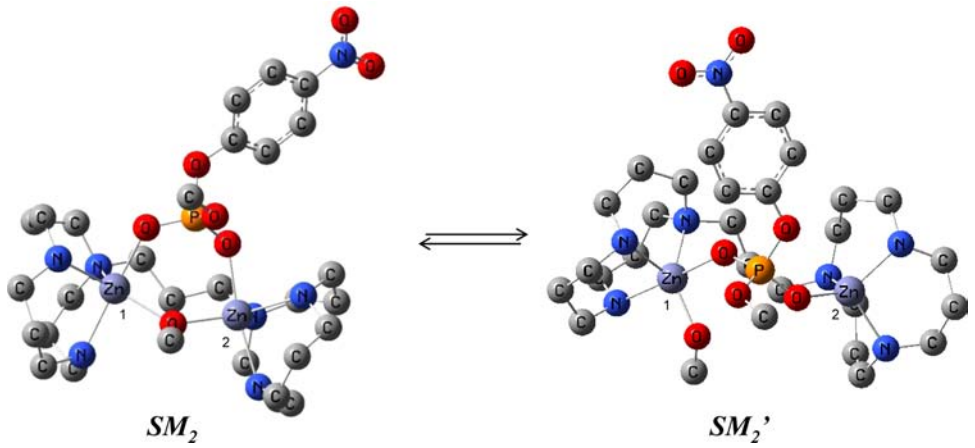

Figure 2. DFT-calculated structures of **2**:**1a** in two forms, SM_2 and SM_2', mainly differing in that the methoxide is coordinated to both or only one $Zn^{(II)}$, respectively. The SM_2' structure is approximately 16.1 kcal mol^{-1} above SM_2. Hydrogen atoms have been omitted for clarity.

dx.doi.org/10.1021/ja4088264 | J. Am. Chem. Soc. 2013, 135, 17209−17222

Scheme 2. A Possible Computed Mechanism for the 1a-Catalyzed Methanolysis of 2 (Mechanism 2A) Involving Direct Nucleophilic Attack of a $Zn^{(II)}$-Bound Methoxide Followed by Rearrangement and Metal-Assisted Leaving Group Departure (Zn Charges Have Been Omitted for Clarity; Relative Free Energies Are Reported in kcal mol^{-1})

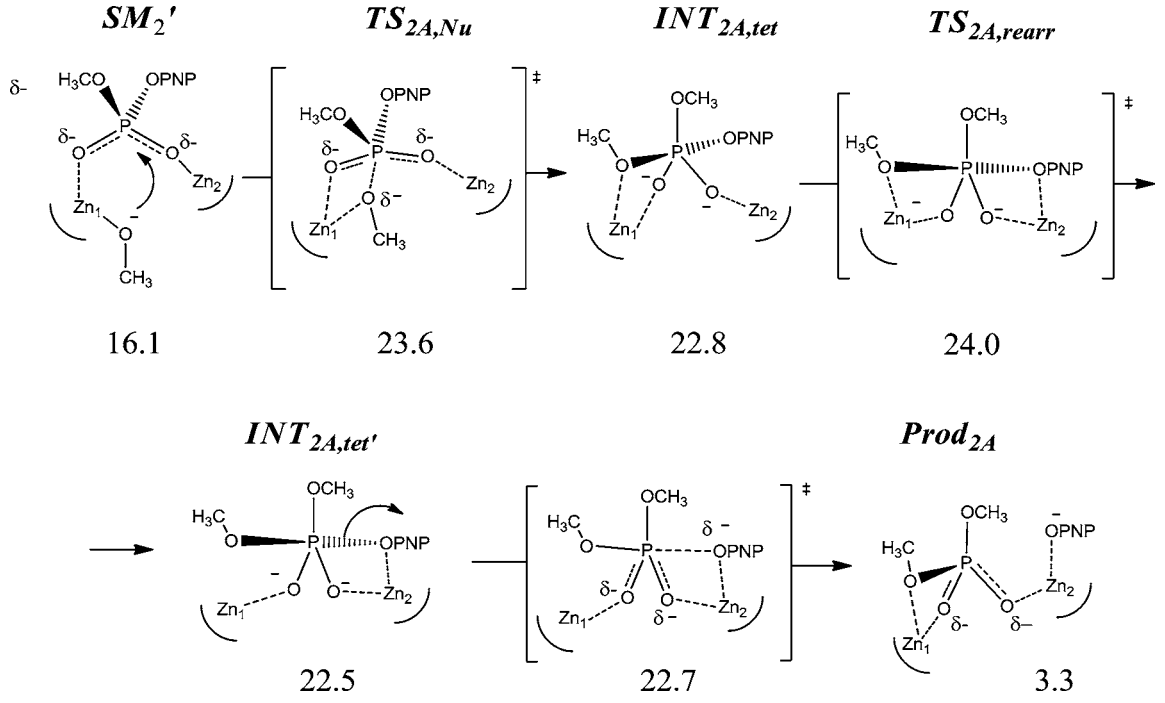

Scheme 3. A Second Possible Computed Mechanism for the 1a-Catalyzed Methanolysis of 2 (Mechanism 2B) Involving Coordination of a Methanol Molecule to the Tetrahedral $Zn^{(II)}_2$ of SM_2' to give INT_{2B} Followed by Nucleophilic Displacement of the Leaving Group by Intramolecular Nucleophilic Attack of $Zn^{(II)}_1$:($^-OCH_3$) via TS_{2B}, Which Has a Free Energy of 18.9 kcal mol^{-1} (Zn Charges Have Been Omitted for Clarity)

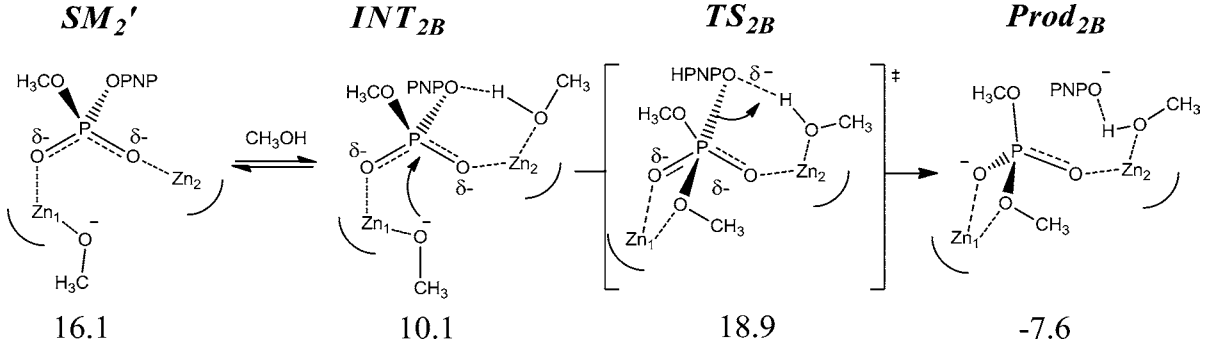

Scheme 4. A Third Possible Computed Mechanism for the 1a-Catalyzed Methanolysis of 2 (Mechanism 2C) Involving Nucleophilic Attack on P Mediated by a General-Base-Promoted Delivery of Methoxide in an Enforced-Concerted[16] Process Having Instantaneous Decomposition of a Short-Lived Phosphorane via Metal-Assisted Leaving Group Departure (Zn Charges Have Been Omitted for Clarity; Relative Free Energies Are Reported in kcal mol^{-1})

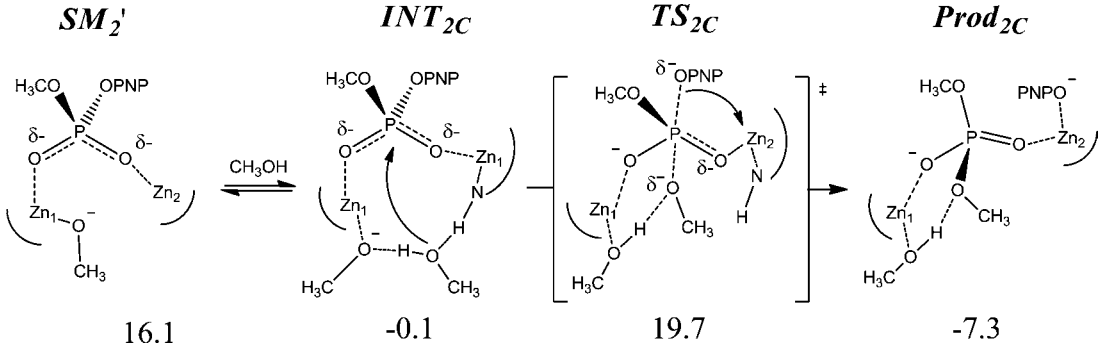

dx.doi.org/10.1021/ja4088264 | J. Am. Chem. Soc. 2013, 135, 17209−17222

Scheme 5. A Fourth Possible Computed Mechanism for the 1a-Catalyzed Methanolysis of 2 (Mechanism 2D) Involving Nucleophilic Attack Mediated by a General-Base Mechanism with Leaving Group Departure Assisted by a Metal-Bound Solvent Molecule (Zn Charges Have Been Omitted for Clarity; Relative Free Energies Are Reported in kcal mol^{-1})

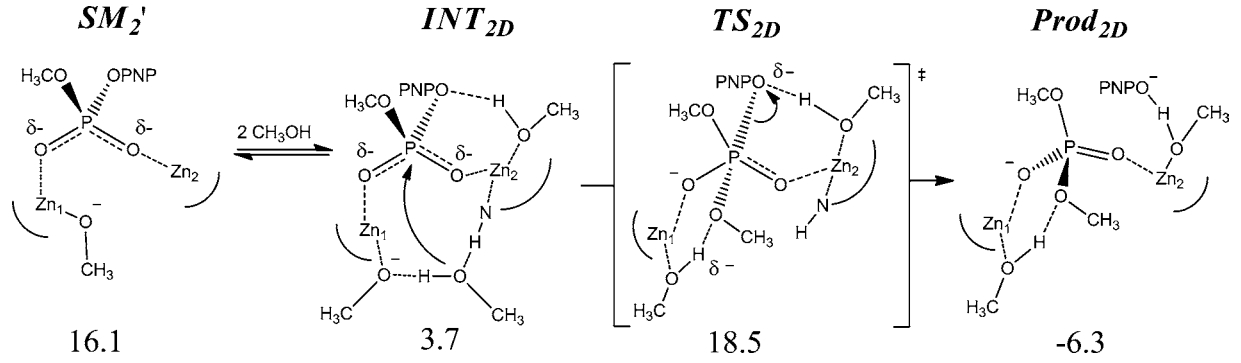

The Scheme 2 mechanism involves nucleophilic attack of the $Zn^{(II)}_1$-coordinated methoxide on the phosphate, which is doubly Lewis acid-activated by the two metal ions, followed by a rearrangement connecting two metal-bound five-coordinate phosphorane intermediates (***INT*$_{2A,tet}$** and ***INT*$_{2A,tet'}$**), leading to subsequent metal-assisted departure of the leaving group. Although several of the intermediates and transition states are within ~2 kcal mol^{-1} of each other, the rate-determining step for this process was found to be the rearrangement via ***TS*$_{2A,rear}$**, in which the former nucleophilic methoxide moiety dissociates from $Zn^{(II)}_1$ and the leaving group coordinates to $Zn^{(II)}_2$ with a TS free energy of 24.0 kcal mol^{-1}.

For the mechanism given in Scheme 3, the stabilization of the methanol-coordinated structure ***INT*$_{2B}$** relative to ***SM*$_2$'** is likely due to both the favorable $Zn^{(II)}_2$–O(H)CH_3 coordination and the addition of a hydrogen-bonding interaction between that methanol and the leaving-group oxygen. The nucleophilic attack of the metal-bound methoxide is concerted with the bound-solvent-assisted departure of the leaving group (***TS*$_{2B}$**) and is associated with a free energy barrier of 18.9 kcal mol^{-1}.

Scheme 4 shows a third possible computed mechanism involving nucleophilic attack on P mediated by general-base-promoted delivery of methoxide by an H–N-associated methanol followed by metal-assisted leaving group departure. In the Scheme 4 process, the association of a hydrogen-bonded methanol molecule to the $Zn^{(II)}_1$-coordinated methoxide and reoptimization resulted in the ***INT*$_{2C}$** structure. During optimization, another hydrogen-bonding interaction developed between the methanol molecule oxygen and an amino proton of the ligand. The oxygen of the *p*-nitrophenoxide leaving group is in the proximity of $Zn^{(II)}_2$ but not directly coordinated ($Zn^{(II)}_2$···OPNP = 3.211 Å). The nucleophilic attack occurs through a general-base mechanism in which proton transfer from methanol to the $Zn^{(II)}_1$-coordinated methoxide is concerted with P–OCH_3 bond formation. Animation of the imaginary vibrational mode associated with this transition state suggested that this transition state largely involves bond formation with little P–OPNP cleavage. The free energy associated with this transition state is 19.7 kcal mol^{-1}. With a stepwise mechanism in mind, we attempted to optimize the corresponding pentacoordinate phosphorane intermediate, but this resulted in shortening of the $Zn^{(II)}_2$–OPNP distance concurrent with barrierless metal-assisted leaving group departure. The overall bond cleavage process appears to be "enforced-concerted",[16] where there is rate-limiting formation of a phosphorane intermediate that has a lifetime too short to exist.

Scheme 5 shows a variant of the mechanism in Scheme 4 in which $Zn^{(II)}_1$:($^-OCH_3$) acts as a general base to assist methanol nucleophilic attack on P concurrent with departure of the leaving group assisted by a $Zn^{(II)}_2$-coordinated solvent molecule. The intermediate prior to nucleophilic attack, ***INT*$_{2D}$**, has two associated methanols and a hydrogen-bonding motif similar to that in ***INT*$_{2C}$** wherein one of the added methanol molecules bridges the methoxide moiety and a ligand amino proton. The ensuing transition state involves concerted general-base proton abstraction, nucleophilic attack, and leaving group departure with an associated free energy of activation of 18.5 kcal mol^{-1}. It should be noted that proton transfer from the $Zn^{(II)}_2$-bound methanol to the leaving group does not occur; rather, the *p*-nitrophenoxide continues accepting that hydrogen bond as it dissociates.

Interestingly, while the TS of the mechanism in Scheme 2 is highest in energy at some 24 kcal mol^{-1}, the limiting TSs of the Scheme 3, 4, and 5 mechanisms have similar free energies (18.9, 19.7, and 18.5 kcal mol^{-1}, respectively). Energetically these cannot be considered sufficiently different to favor one process over another, but all are close to the experimentally measured value[9] (19.3 kcal mol^{-1}). Relevant structural information for the calculated transition states and intermediates of the above four mechanisms are shown in Table 1. Of particular interest is the $Zn^{(II)}_1$···$Zn^{(II)}_2$ interatomic distance, which expands from 3.8 Å in ***SM*$_2$** to over 5.2 Å in all of the subsequent intermediates and transition states, indicating the flexibility required of the transforming complex during the chemical steps. Transition-state geometries are shown in Figure 3.

c. 1a-Catalyzed Cyclization of 3. Possible mechanisms for the cyclization of the RNA model **3** were also explored. These echo those described above for the cleavage of **2** in that they can involve direct nucleophilic attack with metal ion assistance or through a general-base mechanism (but this time generating a 2-propyloxy nucleophile) as well as assistance of leaving group departure involving metal-bound solvent or metal alone. However, prior to the bond formation/breaking events with this substrate, a series of rearrangement steps occurs wherein the pendant 2-hydroxypropyl group of the substrate becomes incorporated with and activated by metal binding or through hydrogen-bonding interactions with $Zn^{(II)}$-bound methanol solvent molecules. The equilibrium presented in Scheme 6 shows the progression from the complex-bound starting

dx.doi.org/10.1021/ja4088264 | J. Am. Chem. Soc. 2013, 135, 17209–17222

Table 1. Selected Structural Data (in Å) from DFT-Calculated Intermediates and Transition States for the 1a-Catalyzed Methanolysis of 2[a]

structure	P–O(Nu)	P–OPNP	$Zn^{(II)}_1$–O(Nu)	$Zn^{(II)}_2$–OPNP	$Zn^{(II)}_1 \cdots Zn^{(II)}_2$
SM_2	3.318	1.653	2.133	4.740	3.799
SM_2'	3.446	1.663	1.967	3.685	5.469
$TS_{2A,Nu}$	2.220	1.753	2.006	3.511	5.245
$INT_{2A,tet}$	1.871	1.790	2.116	3.369	5.191
$TS_{2A,rearr}$	1.846	1.765	2.212	2.664	5.258
$INT_{2A,tet'}$	1.797	1.831	3.461	2.300	5.214
$TS_{2A,LG}$	1.719	1.980	3.509	2.075	5.234
INT_{2B}	3.591	1.668	1.962	3.900	5.557
TS_{2B}	2.219	1.809	2.005	3.743	5.366
INT_{2C}	3.964	1.659	4.254	4.103	5.514
TS_{2C}	2.053	1.804	3.511	3.216	5.511
INT_{2D}	3.921	1.677	4.201	4.028	5.576
TS_{2D}	2.204	1.804	3.516	3.836	5.663

[a]Distances related to the nucleophile are measured from the oxygen of the nucleophilic entity (metal bound CH_3O^- or hydrogen bonded CH_3OH).

material **3**, SM_3, to the two intermediates through which nucleophilic attack can occur, one with metal assistance ($INT_{3,MA}$) and the other through a general-base mechanism ($INT_{3,GB}$). Here, the substrate's propanol group coordinates first to the metal-bridging methoxide to form the transient intermediate SM_3'. This structure disproportionates through either a loosening of the $Zn^{(II)}_2$–($^-OCH_3$) coordination (ΔG_{corr} = 11.7 kcal mol^{-1}; Figure 4) leading to $INT_{3,GB}$ or through a simultaneous $Zn^{(II)}_1$ exchange of its formerly bridged methoxide for a pendant propanol/propoxide (TS_3', ΔG_{corr} = 9.9 kcal mol^{-1}) leading to $INT_{3,MA}$. The mechanism of the departure of methanol in the $SM_3'' \rightleftarrows INT_{3,MA}$ process was not explicitly modeled. Also worthy of note in Scheme 6 is the $INT_{3,min}$ structure, which features the pendant propanol coordinated through hydrogen-bonding interactions to a metal-bound methanol molecule and an amino proton of the ligand. The free energy of this structure relative to SM_3 is −4.0 kcal mol^{-1}, and it corresponds to the minimum-energy conformation available throughout the catalytic process. Structural information for these intermediates and transition states is shown in Table 2.

Several modes of nucleophilic attack can potentially arise from the intermediates participating in the equilibrium described above. These resemble the ones described for the catalyzed reactions of the DNA model **2** in that they can involve nucleophilic attack with metal assistance or through a general-base mechanism as well as the assistance of leaving group departure aided by metal ion or through hydrogen-bonding interactions with a metal-bound solvent molecule. Four of these are shown in Schemes 7–10, in which all of the free energies (ΔG_{corr}) are reported relative to that of the SM_3 structure.

As shown in Scheme 7, the direct closure of the hydroxypropyl oxygen and phosphorus interatomic distance in structure $INT_{3,MA}$ results in a nucleophilic-attack transition state with $\Delta G^{\ddagger}$ = 10.0 kcal mol^{-1}, leading to a phosphorane

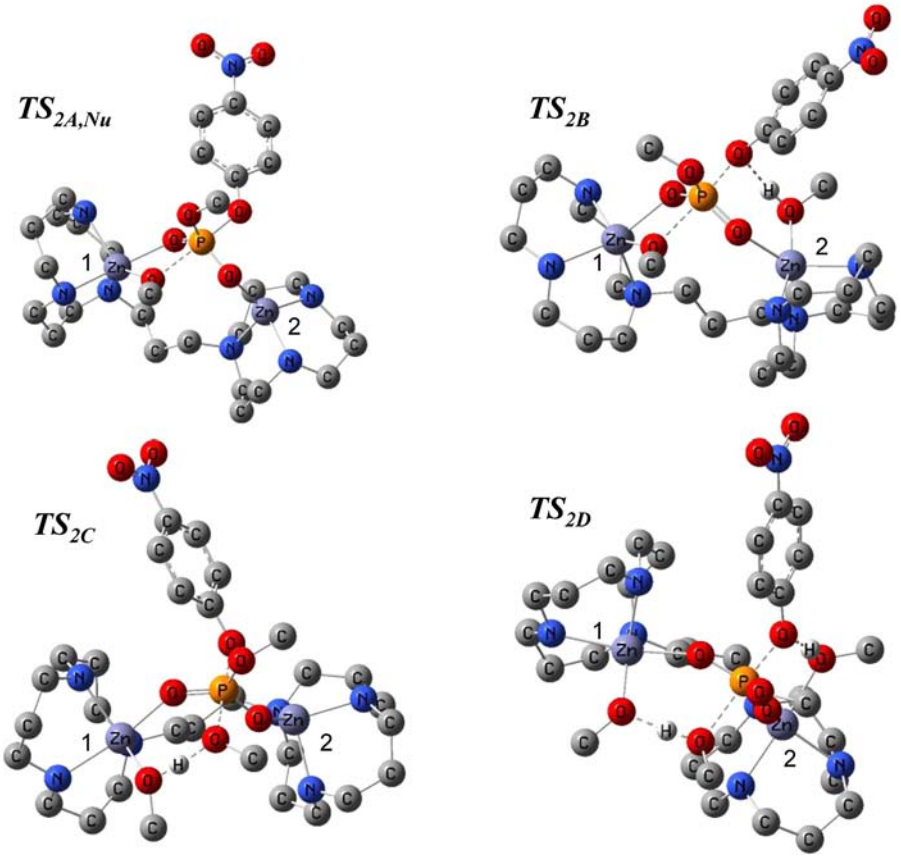

Figure 3. DFT-optimized transition states for the nucleophilic attack steps for the **1a**-catalyzed methanolysis of **2**. Nonrelevant hydrogen atoms have been omitted for clarity.

dx.doi.org/10.1021/ja4088264 | J. Am. Chem. Soc. 2013, 135, 17209–17222

Scheme 6. Mechanisms for the Integration and Activation of the Nucleophilic Pendant 2-Hydroxy Group of Substrate 3 into the Substrate-Bound Complex of 1a

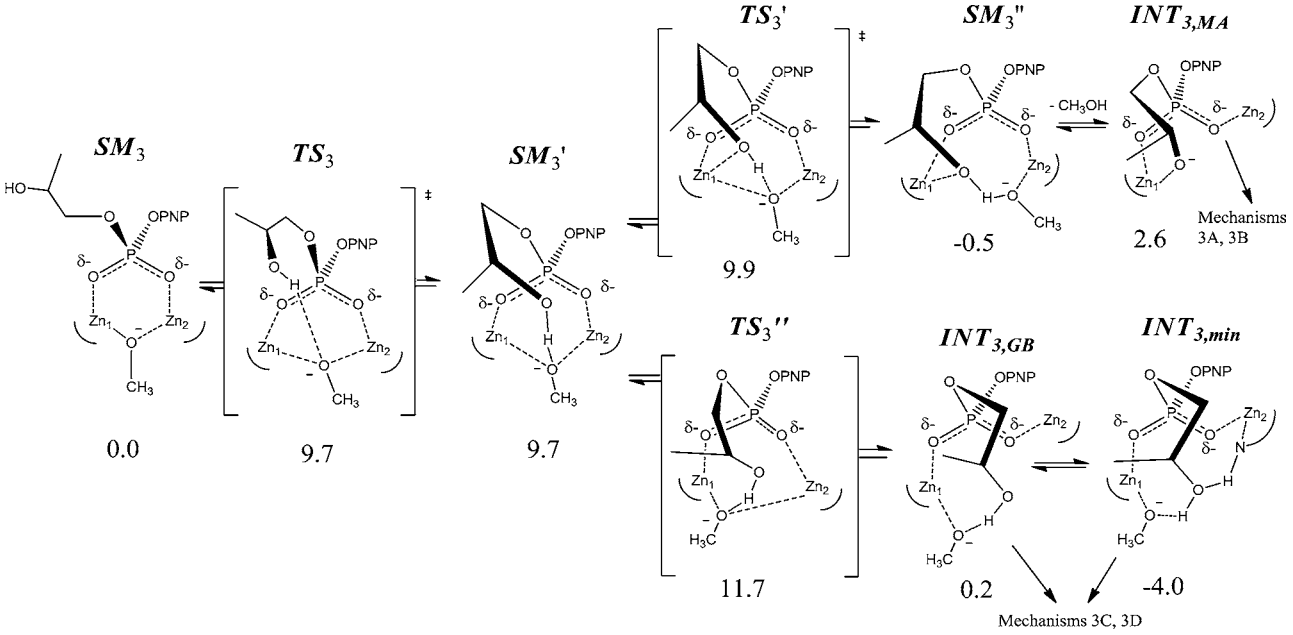

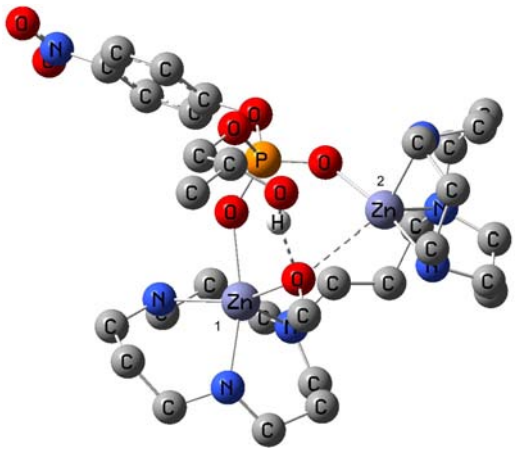

Figure 4. DFT-calculated structure of TS_3'' for the rate-determining step in the integration of the pendant propoxide anion into **1a** (Zn charges have been omitted for clarity).

Table 2. Selected Structural Data (in Å) from DFT-Calculated Intermediates and Transition States for the 1a-Catalyzed Cyclization of 3[a]

structure	P–O(Nu)	P–OPNP	$Zn^{(II)}_1$–O(Nu)	$Zn^{(II)}_2$–OPNP	$Zn^{(II)}_1 \cdots Zn^{(II)}_2$
SM_3	4.277	1.658	5.669	4.707	3.639
TS_3	3.520	1.648	4.569	4.497	3.886
SM_3'	3.346	1.644	4.356	4.518	3.910
TS_3'	3.350	1.649	2.421	4.784	4.171
SM_3''	2.940	1.660	3.971	4.651	4.834
$INT_{3,MA}$	3.356	1.650	1.965	4.460	5.285
TS_3''	3.478	1.645	4.342	4.481	4.238
$INT_{3,GB}$	3.356	1.655	4.030	3.958	5.635
$INT_{3,min}$	3.441	1.652	4.018	4.416	5.518
$TS_{3A,Nu}$	2.246	1.732	2.039	3.822	5.271
$INT_{3A,tet}$	1.876	1.814	2.192	3.899	5.298
$TS_{3A,rearr}$	1.866	1.825	2.283	2.530	5.301
INT_{3B}	3.158	1.673	1.977	3.832	5.574
TS_{3B}	2.339	1.742	2.024	3.788	5.382
$TS_{3C,Nu}$	2.201	1.741	3.590	3.540	5.476
$INT_{3C,tet}$	1.779	1.922	3.577	3.158	5.574
$TS_{3C,LG}$	1.764	1.993	3.589	2.198	5.362
INT_{3D}	3.197	1.661	3.952	4.372	5.572
TS_{3D}	2.301	1.751	3.602	3.820	5.705

[a]Distances related to the nucleophile are measured from the oxygen of the nucleophilic alkoxide.

intermediate. The leaving group oxygen is situated 3.899 Å from $Zn^{(II)}_2$, indicating that a rearrangement similar to that in Mechanism 2A is required to associate the leaving group oxygen and $Zn^{(II)}_2$, resulting in spontaneous P–OLG scission. This rearrangement/leaving group departure step is associated with a $\Delta G^{\ddagger}$ of 12.2 kcal mol^{-1} relative to SM_3.

In Scheme 8 is portrayed a direct nucleophilic attack of the $Zn^{(II)}_1$-coordinated propoxy group that occurs when a methanol molecule becomes coordinated to $Zn^{(II)}_2$. Once the latter is hydrogen-bonded to the leaving group oxygen, nucleophilic attack is concerted with hydrogen-bonding-assisted leaving group departure. This process has a free energy barrier of 9.0 kcal mol^{-1}.

Scheme 9 shows a mechanism in which the $Zn^{(II)}_1$-bound methoxide acts as a general base to facilitate attack of the propanol group through a stepwise process forming a phosphorane intermediate, with proton transfer/bond formation being rate-limiting (ΔG_{corr} = 8.7 kcal mol^{-1}). Leaving group departure from the resulting phosphorane intermediate ($INT_{3C,phos}$) proceeds with the assistance of $Zn^{(II)}_2$.

In Scheme 10, the addition of a methanol molecule bridging the $Zn^{(II)}_2$ ion and the leaving group oxygen causes the $Zn^{(II)}_1$:methoxide general-base-promoted nucleophilic attack of the propanol group to become a concerted process. The transition state for this process is associated with a free energy of 8.4 kcal mol^{-1}.

All of the transition state structures for nucleophilic attack on **3** are shown in Figure 5. As shown in the calculated

dx.doi.org/10.1021/ja4088264 | J. Am. Chem. Soc. 2013, 135, 17209–17222

Scheme 7. A Possible Mechanism for the 1a-Catalyzed Cyclization of 3 (Mechanism 3A) Involving Direct Nucleophilic Attack of a $Zn^{(II)}$-Bound Pendant Alkoxide and Metal-Assisted Leaving Group Departure (Zn Charges Have Been Omitted for Clarity; Free Energies Are Reported in kcal mol^{-1})

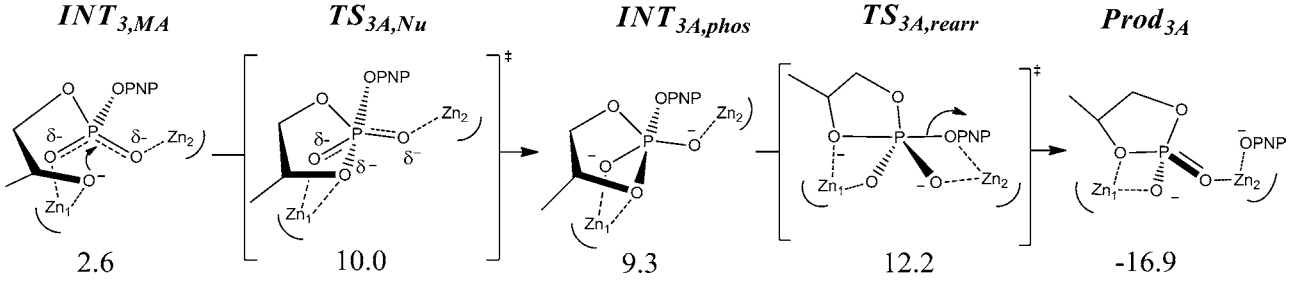

Scheme 8. A Second Possible Mechanism Modeled for the 1a-Catalyzed Cyclization of 3 (Mechanism 3B) Involving Nucleophilic Attack of Metal-Coordinated Pendant Alkoxide with Concerted Solvent-Assisted Leaving Group Departure (Zn Charges Have Been Omitted for Clarity)

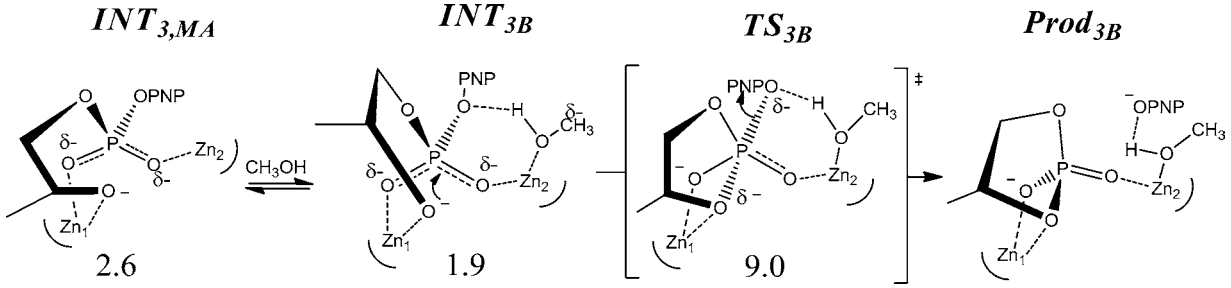

Scheme 9. A Third Possible Mechanism Modeled for the 1a-Catalyzed Cyclization of 3 (Mechanism 3C) Involving Nucleophilic Attack through a General-Base Mechanism and Metal-Assisted Leaving Group Departure (Zn Charges Have Been Omitted for Clarity)

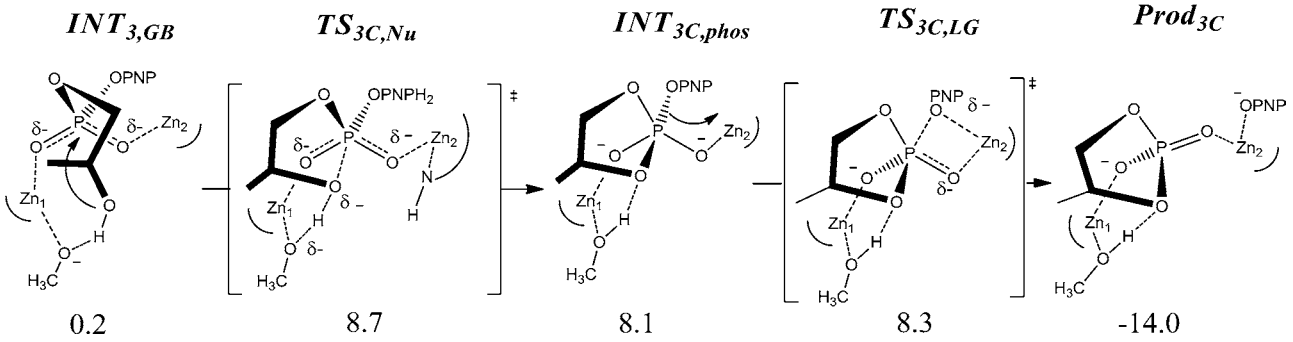

Scheme 10. A Fourth Possible Mechanism Modeled for the 1a-Catalyzed Cyclization of 3 (Mechanism 3D) Involving Nucleophilic Attack through a General-Base Mechanism in Concert with Leaving Group Departure Assisted by Zn_2-Coordinated Solvent (Zn Charges Have Been Omitted for Clarity)

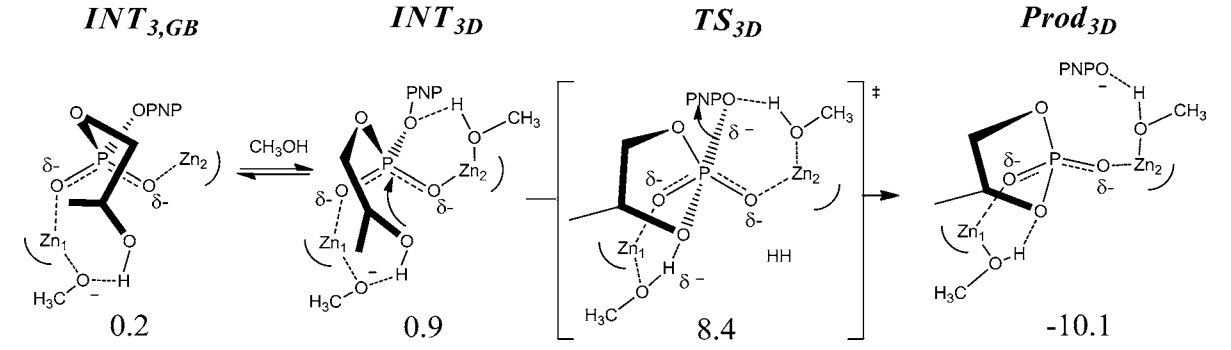

mechanisms for the **1a**-catalyzed methanolysis of DNA analogue **2**, the barrier associated with mechanism 3A for cyclization of RNA analogue **3** is significantly larger, but the rate-limiting transition-state structures occurring during the

dx.doi.org/10.1021/ja4088264 | J. Am. Chem. Soc. 2013, 135, 17209−17222

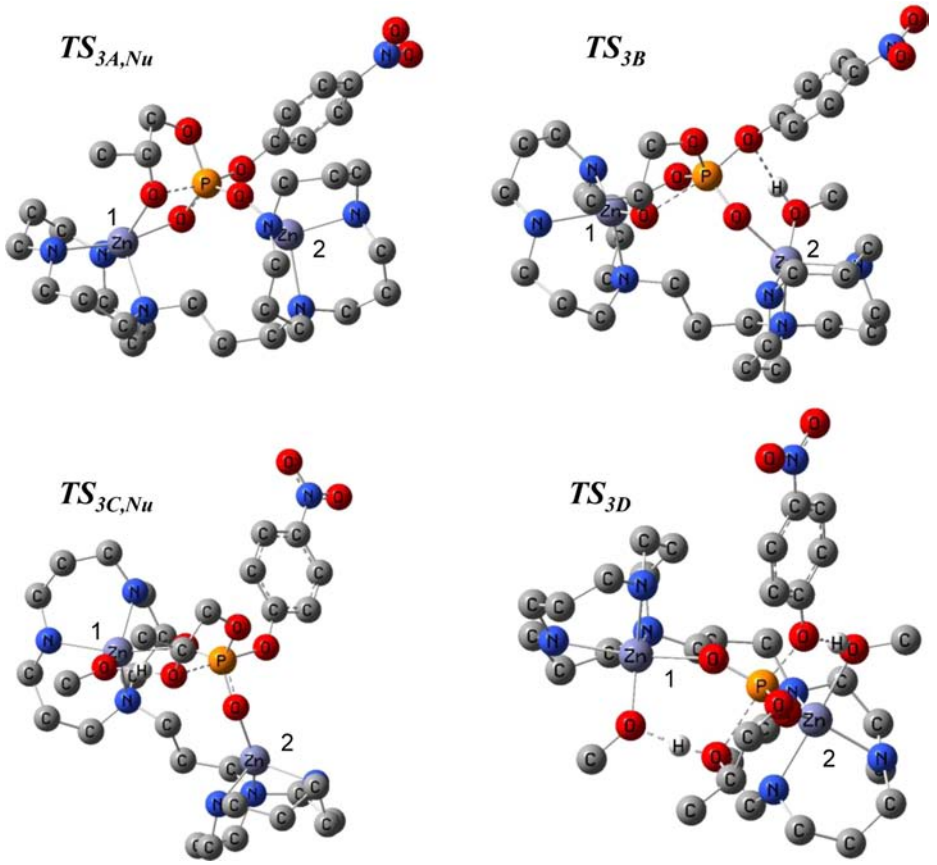

Figure 5. DFT-optimized transition states for the nucleophilic attack steps for the **1a**-catalyzed methanolysis of **3**. Nonrelevant hydrogen atoms have been omitted for clarity.

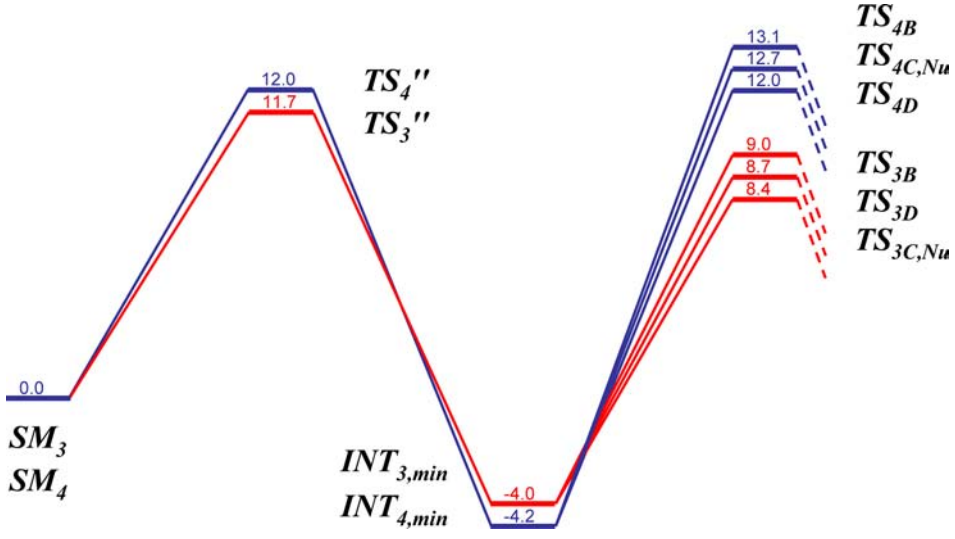

Figure 6. Free energy profile (drawn to scale; values in kcal mol^{-1}) for the rate-determining processes associated with the **1a**-catalyzed methanolyses of substrates **3** and **4**.

chemical steps of mechanisms 3B, 3C, and 3D have considerably lower energies (9.0, 8.7, and 8.4 kcal mol^{-1}, respectively). In fact, these three mechanisms provide pathways for the reaction that are lower in free energy than that of the initial rearrangement required to activate the 2-hydroxypropyl nucleophile (***TS***$_3$″, 11.7 kcal mol^{-1}); this step is considered rate-limiting for any of these processes. If the ***INT***$_{min}$ structure is taken as the ground-state structure for the bound substrate, the differences in free energy of activation related to the catalyzed process are 13.0 kcal mol^{-1} (3B), 12.7 kcal mol^{-1} (3C), and 12.4 kcal mol^{-1} (3D), similar to the experimentally predicted value[17] of 12.8 kcal mol^{-1}.

d. 1a-Catalyzed Cyclization of 4. With the catalyzed cyclization mapped for substrate **3** and the assumption that the same mechanism(s) is (are) operating with the same potential rate-limiting steps, the relevant intermediates and transition

dx.doi.org/10.1021/ja4088264 | J. Am. Chem. Soc. 2013, 135, 17209−17222

Table 3. Free Energies for the Rate-Limiting Steps and the Roles of $Zn^{(II)}_1$ and $Zn^{(II)}_2$ in the Cleavage of Substrates 2 and 3 Promoted by 1a

substrate (scheme)	TS ($\Delta G^{\ddagger}$ in kcal mol^{-1})	role of $Zn^{(II)}_1$	role of $Zn^{(II)}_2$	nucleophilic reaction
2 (2)	TS_{2A} (24)	Zn_1:($^-OCH_3$) nucleophile	direct LGA[a]	stepwise
2 (3)	TS_{2B} (18.9)	Zn_1:($^-OCH_3$) nucleophile	Zn_2–($HOCH_3$) H-bonding LGA[b]	concerted
2 (4)	TS_{2C} (19.7)	Zn_1:($^-OCH_3$) general base	no LGA	concerted
2 (5)	TS_{2D} (18.5)	Zn_1:($^-OCH_3$) general base	Zn_2–($HOCH_3$) H-bonding LGA[b]	concerted
3 (7)	$TS_{3A,rear}$ (12.2) {16.2}[c]	Zn_1:($^-$OPr)[d] nucleophile	direct LGA[a]	stepwise
3 (8)	TS_{3B} (9.0) {13.0}[c]	Zn_1:($^-$OPr)[d] nucleophile	Zn_2–($HOCH_3$) H-bonding LGA[b]	concerted
3 (9)	$TS_{3C,Nu}$ (8.7) {12.7}[c]	Zn_1:($^-OCH_3$)[e] general base	direct LGA[a]	stepwise
3 (10)	TS_{3D} (8.4) {12.4}[c]	Zn_1:($^-OCH_3$)[e] general base	Zn_2–($HOCH_3$) H-bonding LGA[b]	concerted

[a]Direct coordination of the leaving group to $Zn^{(II)}_2$ to provide leaving group assistance. [b]$Zn^{(II)}_2$–($HOCH_3$) provides hydrogen bonding to assist the departure of the leaving group. [c]Energies in braces were computed relative to $INT_{3,min}$ (Scheme 6), which is the lowest-energy bound form of the catalyst:3 complex. [d]$Zn^{(II)}_1$:($^-$O-propyl) is delivered to P as a nucleophile. [e]$Zn^{(II)}_1$:($^-OCH_3$) acts as a general base to deprotonate the propanol concurrent with the latter's nucleophilic attack on P.

states of the catalyzed methanolysis of the less activated, phenoxy-containing substrate **4** were calculated. A comparison of the energies for the rate-limiting processes is shown in Figure 6. Here we see a trend developing in that the barriers associated with the nucleophilic attack are generally higher than that of the rate-determining pendant hydroxide integration step. Thus, it is plausible that nucleophilic attack becomes limiting for substrates with poor leaving groups. The calculated free energies of activation for the chemical process (with $INT_{4,min}$ as the ground state) are 16.2, 16.9, and 17.3 kcal mol^{-1}, which are similar to the experimentally determined value[2a] for the cleavage of the **1a**:**4** complex (16.8 kcal mol^{-1}).

DISCUSSION

Table 3 provides a summary of the DFT-derived data for the rate-limiting steps for the chemical cleavage of substrates **2** and **3** along with the role of $Zn^{(II)}_1$:($^-$OR) as a general base or nucleophile, the role of $Zn^{(II)}_2$ in assisting leaving group departure by direct coordination or hydrogen bonding via $Zn^{(II)}_2$–($HOCH_3$), and a designation of whether the overall reaction involves a concerted or stepwise process. It should be noted that for the cleavage of **2** the rate-limiting steps are those associated with chemical processes involving bond making and breaking, while for **3** the rate-determining step is a rearrangement that repositions the hydroxypropyl group prior to the chemical steps of cyclization.

a. Experimental Mechanistic Details To Be Reconciled with the DFT Computations. Prior to considering the mechanistic implications of the DFT calculations, we present a brief description of the mechanistic results derived from prior experimental studies.[2,9] Six of these are the following:

1. The stoichiometry of the active form of the catalyst is **1a**, which has maximum activity at a "pH" of 9.8 ± 0.2 in methanol. The methoxide is thought to bridge the two $Zn^{(II)}$ ions on the basis of the X-ray diffraction structure for the corresponding hydroxide complex.[2a]

2. Plots of the observed rate constant (k_{obs}) for the formation of product from **2** and other aryl methyl phosphates versus [**1a**] in all cases show downward curvature suggestive of saturation binding, analyzed in terms of the K_m (substrate/catalyst dissociation constant) and k_{cat} (the rate constant for decomposition of the **1a**:substrate complex.[2a,9] The same is true for almost all derivatives of 2-hydroxypropyl aryl phosphates except those with very good leaving groups such as **3** (vide infra).[2a,d] A plot of k_{obs} for the formation of product from **3** versus [**1a**] is linear with a gradient of 275 000 M^{-1} s^{-1} and shows no evidence of downward curvature indicative of saturation binding. These data have been interpreted as indicating that there is a rearrangement of the initially formed complex to form an activated complex (as in eq 3) in which the subsequent chemical steps for cyclization of ($HOCH(CH_3)$-CH_2O)(ArO)PO_2^- substrates having very good ArO^- leaving groups are faster than the rearrangement.[2a,d,9] With substrates having poorer leaving groups, the binding and rearrangement steps of the **1a**:substrate complex are at equilibrium, and the rate-limiting step becomes a chemical one that depends on the "pH" (in methanol) of the aryloxy leaving group.

3. The Brønsted plot of log k_{cat} versus "pH" (in methanol) for catalyzed methanolysis of the aryloxy derivatives of **2** is linear with a gradient (Brønsted β) of −0.59 ± 0.03.[2f] If the reaction is considered to be concerted, these data are consistent with an associative transition state with a rate-limiting step in which the cleavage of the aryloxy–P bond has progressed about 32%. The available data are also consistent with a two-step process, with the first step being rate-limiting.

4. The Brønsted plot of log k_{cat} versus "pH" (in methanol) for cyclization of the aryloxy derivatives of **3** (having leaving groups where the pK_a values are higher than that of *p*-nitrophenol) is linear with a gradient of −0.97 ± 0.05. If the cleavage reaction is concerted, the data are consistent with a looser transition state than with the aryl methyl derivatives, having about 53% cleavage of the aryloxy–P bond at the transition state.[2a] These data are also consistent with a two-step process with the first step being rate-limiting, although the large negative value of the gradient suggests considerable loosening of the departing group in the transition state, which would be more consistent with a concerted process.

5. The k_{cat} term for the catalyzed cyclization reaction of **3** cannot be measured directly, but it is assumed that it would lie on the same Brønsted line as for other aryloxy derivatives of **3**.[2a] Following this relationship, one computes a decomposition rate constant for the **1a**:**3** complex of k^3_{cat} = 2300 s^{-1}, which yields a computed $\Delta G^{\ddagger}$ (25 °C) of 12.8 kcal mol^{-1} for the rate-limiting step.[8,9] For comparison purposes, the k_{cat} value for the catalyzed cleavage of *O*-2-hydroxypropyl *O*-phenyl phosphate is 3.1 s^{-1}, for which $\Delta G^{\ddagger}$ is 16.8 kcal mol^{-1}.[2a] The experimental k^2_{cat} value is 4.15 × 10^{-2} s^{-1}, for which the $\Delta G^{\ddagger}$ (25 °C) value is 19.3 kcal mol^{-1}.[9] For comparison purposes, the k_{cat} value for the catalyzed cleavage of *O*-methyl *O*-phenyl phosphate is 5.3 × 10^{-4} s^{-1}, for which $\Delta G^{\ddagger}$ is 21.9 kcal mol^{-1}.[2f]

6. There are questions about the mode of deprotonation of the hydroxypropyl group in the cyclization of **3** when bound to

1a. In the case of the cyclization of **3** promoted by complex **5**, Richard and Morrow[4d] have presented convincing evidence that the reaction in water is subject to specific base catalysis with equilibrium deprotonation of the hydroxypropyl group occurring prior to rate-limiting nucleophilic attack on P. On the other hand, the cyclization of **3** promoted by **1a** and **1b**[2g] cannot be subject to specific base catalysis since analysis of the states of ionization at the "pH" values in methanol or ethanol where high activity is observed suggests that there is not enough free alkoxide in solution to achieve the required rates without the proton transfer exceeding the diffusion limit.[18] Thus, these cyclization reactions are considered to be subject to general base catalysis in the light alcohols.

b. 1a-Catalyzed Methanolysis of DNA Model 2. The DFT investigation into the catalyzed methanolysis of **2** provides some new mechanistic insights that complement and are consistent with the experimental findings presented above. Before nucleophilic attack can proceed, as shown in Scheme 1, the bridging methoxide dissociates from one of the $Zn^{(II)}$ ions and is coordinated only with $Zn^{(II)}_1$. This process is endothermic by 16.1 kcal mol^{-1} and not only increases the nucleophilicity and basicity of the methoxide but allows the complex to expand and place $Zn^{(II)}_2$ in such a position that it may ultimately assist leaving group departure. The geometric requirements of both a $Zn^{(II)}$-assisted nucleophilic methoxide attack and $Zn^{(II)}$-assisted leaving group departure (Scheme 2, mechanism 2A) cannot be met simultaneously, as the required $Zn^{(II)}$–$Zn^{(II)}$ locations could not be adopted by the catalyst. For mechanism 2A to proceed past the nucleophilic attack step, a higher-energy rearrangement involving concurrent nucleophile–$Zn^{(II)}_1$ dissociation and leaving group–$Zn^{(II)}_2$ association must occur. Conveniently, if a methanol molecule becomes coordinated to $Zn^{(II)}_2$ and enters into a hydrogen-bonding interaction with the leaving group's oxygen, the nucleophilic attack of the $Zn^{(II)}_1$-bound methoxide can proceed with leaving group assistance provided by a $Zn^{(II)}_2$-bound solvent acting as a general acid or as a hydrogen-bonding stabilizer (Scheme 3, mechanism 2B). The attack of a solvent methanol that is activated by the $Zn^{(II)}_1$:($^-OCH_3$) through a general-base mechanism allows the leaving group oxygen to remain in proximity to $Zn^{(II)}_2$ so that its departure can be assisted (Scheme 4, mechanism 2C). A mechanism involving two additional methanol molecules (Scheme 5, mechanism 2D) was also envisioned, and the free energy requirements for mechanisms 2B, 2C, and 2D are similar, with each being consistent with the experimentally determined k^2_{cat} value, for which the $\Delta G^{\ddagger}$ (25 °C) value is 19.3 kcal mol^{-1}.[2a] From the compendium in Table 3, mechanisms 2B, 2C, and 2D all involve a concerted displacement of the leaving group, but the details differ in that $Zn^{(II)}_1$:($^-OCH_3$) acts either as a nucleophile or a general base (if there is a second methanol molecule). The $Zn^{(II)}_2$ either has no catalytic role beyond that of Lewis acid activation of the bound phosphate (2C) or, when bound to a coordinated methanol, assists the departure of the leaving group in mechanisms 2B and 2D through hydrogen bonding, such assistance providing the lowest-energy transition states (18.9 and 18.5 kcal mol^{-1} respectively). It is important to note that the availability of each of mechanisms 2B, 2C, and 2D depends strictly on the flexibility of the ligand to permit the $Zn^{(II)}$ ions to separate (from 3.799 Å apart in SM_2 to more than 5 Å in later steps), allowing them to assume their distinct catalytic roles.

c. 1a-Catalyzed Cyclization of RNA Models 3 and 4. The cyclizations of the RNA model substrates **3** and **4** are complicated by the process through which the pendant alkoxide group is incorporated into and activated by the dinuclear $Zn^{(II)}$ catalyst. The experimental plot of k^3_{obs} versus [**1a**] does not show evidence of curvature to at least 0.7 mM catalyst, suggesting that we are far from saturation binding of **3** at this concentration.[2a,d,17] On the other hand, the DFT calculations for this process assume that one starts with the **3**:**1a** complex, so all of the conclusions made on the basis of the calculations refer to this ground state. As shown in Scheme 6, the process by which the pendant alkoxide group becomes ligated to $Zn^{(II)}_1$ of the catalyst is of relatively high energy for the highly activated substrate **3** and at equilibrium leads to a relatively stable intermediate structure $INT_{3,min}$, which is considered to be the ground state for subsequent chemical steps (at standard state, $INT_{3,min}$ is −4.0 kcal mol^{-1} lower than the initially bound form SM_3). As was seen with the DNA model **2**, there are three plausible competing mechanisms involving similar solvent methanol placements for the phosphate cleavage steps of **3** and **4**, and the barriers associated with these mechanisms are similar to the extrapolated value derived for the k^3_{cat} process (12.8 kcal mol^{-1}).[2a] In each case, there is a large degree of flexibility permitted by the ligand to allow the two $Zn^{(II)}$ ions to rearrange in order to accommodate the geometric requirements for assisting both nucleophilic attack and leaving group departure. For mechanism 3A, shown in Scheme 7, there is a stepwise nucleophilic attack of the $Zn^{(II)}_1$:($^-OCH_3$) with a $\Delta G^{\ddagger}$ of 10 kcal mol^{-1} leading to the phosphorane intermediate $INT_{3A,phos}$, which then undergoes a rate-limiting step of rearrangement via $TS_{3A,rear}$ with concerted coordination of the leaving group to $Zn^{(II)}_2$ and cleavage of the P–OAr bond ($\Delta G^{\ddagger}$ = 12.2 kcal mol^{-1}; 16.2 kcal mol^{-1} relative to $INT_{3,min}$). Because of the high energy of $TS_{3A,rear}$, mechanism 3A is considered less likely than the remaining three discussed below.

Mechanism 3B (Scheme 8) involves $Zn^{(II)}_1$:($^-OCH_3$) nucleophilic attack on P in concert with $Zn^{(II)}_2$–($HOCH_3$) hydrogen-bonding-assisted departure of the aryloxy group, for which the TS_{3B} energy is 9.0 kcal mol^{-1} (13 kcal mol^{-1} relative to $INT_{3,min}$).

Mechanism 3C (Scheme 9) involves a stepwise process wherein $Zn^{(II)}_1$:($^-OCH_3$) is involved in rate-limiting general-base deprotonation of the pendant hydroxypropyl group to assist its nucleophilic attack on P to form $INT_{3C,phos}$ ($\Delta G^{\ddagger}$ = 8.7 kcal mol^{-1}; 12.7 kcal mol^{-1} relative to $INT_{3,min}$). Subsequent breakdown of the latter occurs with direct assistance of leaving group departure by $Zn^{(II)}_2$.

Mechanism 3D (Scheme 10) is a variant of mechanism 3C with the inclusion of an additional methanol on $Zn^{(II)}_2$. The concerted displacement involves a general base role for $Zn^{(II)}_1$:($^-OCH_3$) and a $Zn^{(II)}_2$–($HOCH_3$) hydrogen-bonding assistance of the departure of the *p*-nitrophenoxy group ($\Delta G^{\ddagger}$ = 8.4 kcal mol^{-1}; 12.4 kcal mol^{-1} relative to $INT_{3,min}$). Relevant to the possibility that the rate-limiting step involves general acid assistance by metal-coordinated solvent or direct association with the metal ion is the study of Mikkola and co-workers, who showed that Zn^{2+} catalysis of the cleavage of RNA phosphodiesters with poorer leaving groups such as alkoxy groups involves general acid catalysis by Zn^{2+}(HOH).[19]

It is notable that DFT computations on the **1a**-promoted cleavage of the less reactive substrate **4** (Figure 6, blue lines) provided evidence for higher computed barriers for TS_4'' than TS_3'', a lower computed energy for $INT_{4,min}$ than $INT_{3,min}$, and

dx.doi.org/10.1021/ja4088264 | J. Am. Chem. Soc. 2013, 135, 17209−17222

higher computed barriers for TS_{4B}, $TS_{4C,Nu}$, and TS_{4D} than for TS_{3B}, $TS_{3C,Nu}$, and TS_{3D}. This is consistent with the experimental observations that the catalyzed cleavage of **4** has higher barriers for the chemical steps involving nucleophilic attack. The experimental data for **4** show that the plot of k_{obs} versus [**1a**] is curved downward, providing evidence of saturation binding, which suggests that one of the later steps in the cleavage reaction is rate-limiting.[2a]

CONCLUSIONS

The **1a**-promoted cleavages of two series of substituted aryl methyl phosphates ($\mathbf{2}_{subst}$) and aryl 2-hydroxypropyl phosphates ($\mathbf{3}_{subst}$) are greatly accelerated relative to the background methoxide-promoted reactions in methanol at 25 °C. Where the catalyst is most active at close to neutral "pH" in methanol, both sets of reactions are accelerated by at least 10^{12} relative to the background processes,[2,9] and very strong catalysis is also seen in ethanol, where the **1b**-promoted cyclizations of $\mathbf{3}_{subst}$ are accelerated by 10^{12} to 10^{14}.[2g] We have speculated[2,9] that the catalytic efficacy arises from a medium effect where the reduced dielectric constant of the light alcohols favors substrate binding and also reduces the energies for processes where charge is being dispersed in the transition state of the cleavage reaction.

The present computational studies indicate that there may be additional important effects not revealed by experiment. After binding of the substrate, the dinuclear system increases its flexibility and can accommodate the changing geometric requirements for placement of the two metal ions in key locations around the transforming phosphodiester to assist the various steps in passing from bound substrate to product. Another possibility, not easily probed by experiment, is the assistance with the departure of the leaving group by $Zn^{(II)}_2$ (either by itself or along with a bound methanol) from the transforming substrate in a concerted or stepwise process. Attempts to understand the profound rate accelerations occasioned by metal-ion-containing phosphodiesterase enzymes have provoked interest in other small-molecule dinuclear complexes (e.g., **5**[4] and those based on 2-picolylamine complexes[5]) that catalyze the hydrolysis of phosphate diesters in water. Although much has been learned about the mechanism of such processes,[3−5] the observed rate accelerations are far less than is possible with **1a** and **1b** in methanol or ethanol. A common structural element of most dinuclear $Zn^{(II)}$ complexes that are active in water is a permanently installed ligand-bound oxyanion bridging group that appears to be necessary for holding the two $Zn^{(II)}$ ions in proximity in aqueous solution.[20] Notably, complexes **1** have poor activity in water,[21a] even in the presence of an equivalent of hydroxide,[21b] but when the solvent is changed to methanol or ethanol we find high activity. In addition, although a *temporarily* bound bridging methoxide or ethoxide is a definite asset for positioning the two $Zn^{(II)}$ ions of complex **1** to accept the phosphodiester substrates, a *permanently* bridging oxyanion is not necessary for proper metal binding to form **1a** or **1b** in alcohol. In fact, such a permanently bound bridging oxyanion is detrimental to optimal catalytic activity, since **6** is 37 000 times less active than **1a** in promoting the cyclization of **3** in methanol.[2b] The reduction in activity was proposed to be due to a decrease in the Lewis acidity of the $Zn^{(II)}$ ions, a larger coordination number imposed on each $Zn^{(II)}$ ion by the permanently bridging oxyanion, and decreased stabilization of the negative charge development in the transition state. However, it now seems likely that the loss of conformational flexibility imposed by the oxyanion bridge must also severely curtail the catalytic activity because optimal binding of the transforming substrate to **6** cannot occur.

Recently, two computational works[6,7] modeled the cyclization of **3** catalyzed by a similar dinuclear Zn complex, **5**, in water. The projected mechanisms for the catalyzed cyclizations in the two studies differ. The report[6] most consistent with the extant experimental results favors a specific-base process where each terminal phosphoryl oxygen atom of **3** binds to a $Zn^{(II)}$ center, the nucleophilic 2-hydroxypropyl group coordinates to one of the $Zn^{(II)}$ ions, and a hydroxide from a deprotonated water molecule coordinates to the other $Zn^{(II)}$ ion. Subsequent formation of a $Zn^{(II)}$-bound 2-propoxy group results in concerted displacement of the *p*-nitrophenoxy group to give the cyclized product. This mechanism is reminiscent of mechanism 3B (Scheme 8), where concerted departure of the leaving group occurs with hydrogen-bonding assistance by the $Zn^{(II)}_2$-coordinated methanol. The second computational study[7] found similar binding of the substrate to the ligand but proposed a general-base-promoted two-step process where a $Zn^{(II)}$-bound ^{-}OH deprotonates the 2-hydroxypropyl group with simultaneous formation of a phosphorane intermediate that subsequently forms the cyclized product. While differing in the mechanistic outcome because of computational differences, the two studies illustrate a common feature stemming from the constrained nature of the geometry of the two Zn ions in **5**: throughout the catalytic process, the inter-$Zn^{(II)}$ distance remains at ∼3.6 Å. This is in stark contrast to the methanolytic process calculated in the present work where the inter-Zn distance varies from ∼3.8 to ∼5.7 Å.

Aside from the flexibility of the ligand system, which adds another dimension to enhancing the catalytic efficacy in small molecules, it is of interest that the computations show that cleavage of each substrate has at least three different mechanisms that are energetically very close to the experimental values along with at least one additional mechanism for each substrate that can probably be discounted as being too high in energy. These mechanisms fall into concerted or stepwise categories and involve different roles for the two metal ions. Aside from providing Lewis acid binding for the substrate, either $Zn^{(II)}_1$:($^{-}OCH_3$) and $Zn^{(II)}_1$:(2-($^{-}$O-propyl)) play the role of direct nucleophiles (on **2** and **3**, respectively) or $Zn^{(II)}_1$:($^{-}OCH_3$) can act as a general base to deprotonate an attacking solvent of the 2-hydroxypropyl group in the case of **3**. On the other hand, $Zn^{(II)}_2$ can either serve as a spectator (after exerting its Lewis acid role) or play an additional active role to provide direct coordination of the departing group or to position a hydrogen-bonding solvent to assist LG departure. Although it might be thought that the computational identification of multiple catalytic mechanisms is a failure of the methodology, we take an alternative view that requires testing, namely, that the flexibility of the system permits alternative pathways that might be advantageous in expanding the scope of substrates accepted for catalytic cleavage, accommodating differences in steric demand, electronic effects, variation in the goodness of leaving group, and substitution patterns.

According Pauling's principles of enzyme catalysis,[22] "the enzyme has a configuration complementary to the activated complex, and accordingly has the strongest power of attraction for the activated complex". It follows that for any catalyst promoting a multistep reaction, each of the steps must be lowered in energy to achieve the overall high rates for the

dx.doi.org/10.1021/ja4088264 | J. Am. Chem. Soc. 2013, 135, 17209−17222

catalytic reaction. Zhang and Houk[23] recently provided a comprehensive analysis of possible enzymatic roles in catalysis, the principles of which are relevant to small-molecule-catalyzed reactions as well. In addition, there is convincing evidence that conformational flexibility is important for substrate and cofactor binding, repositioning of active-site residues along the catalytic pathway, and product release, but there is still considerable debate as to the importance of dynamical protein flexibility as an important feature along the chemical pathway leading from bound substrate to products.[24]

Conformational restriction of access of the reagent to the substrate is an important aspect of small-molecule catalysts for multistep organic and other transformations that sterically enable enantioselective or -specific reactions such as Diels–Alder, epoxidations, alkene hydrogenation, aldol condensations, reductions, and organozinc additions to carbonyls[25] rather than solvolytic processes. The present computational results for the **1a**-promoted solvolytic reactions of phosphodiesters **2**–**4** imply that here too conformational flexibility of a dinuclear catalyst during its solvolytic transformation of a bound phosphodiester is a key element in providing fast reactions in a biomimetic transesterification process.

■ ASSOCIATED CONTENT

Supporting Information

Atomic positions of calculated structures. This material is available free of charge via the Internet at http://pubs.acs.org.

■ AUTHOR INFORMATION

Corresponding Authors

christophermaxwell3@gmail.com
Nicholas.Mosey@chem.queensu.ca
rsbrown@chem.queensu.ca

Notes

The authors declare no competing financial interest.

■ ACKNOWLEDGMENTS

The authors gratefully acknowledge the financial support of NSERC (Canada) and Queen's University. In addition, they acknowledge the preliminary calculations of Mr. Jason Stephens as well as ongoing discussions with Dr. Alexei A. Neverov.

■ REFERENCES

(1) Chin, J. *Acc. Chem. Res.* **1991**, *24*, 145.

(2) (a) Bunn, S. E.; Liu, C. T.; Lu, Z.-L.; Neverov, A. A.; Brown, R. S. *J. Am. Chem. Soc.* **2007**, *129*, 16238. (b) Mohamed, M. F.; Neverov, A. A.; Brown, R. S. *Inorg. Chem.* **2009**, *48*, 11425. (c) Lu, Z.-L.; Liu, C. T.; Neverov, A. A.; Brown, R. S. *J. Am. Chem. Soc.* **2007**, *129*, 11642. (d) Neverov, A. A.; Lu, Z.-L.; Maxwell, C. I.; Mohamed, M. F.; White, C. J.; Tsang, J. S. W.; Brown, R. S. *J. Am. Chem. Soc.* **2006**, *128*, 16398. (e) Liu, C. T.; Neverov, A. A.; Brown, R. S. *J. Am. Chem. Soc.* **2008**, *130*, 13870. (f) Neverov, A. A.; Liu, C. T.; Bunn, S. E.; Edwards, D.; White, C. J.; Melnychuk, S. A.; Brown, R. S. *J. Am. Chem. Soc.* **2008**, *130*, 6639. (g) Liu, C. T.; Neverov, A. A.; Brown, R. S. *J. Am. Chem. Soc.* **2008**, *130*, 16711. (h) Liu, C. T.; Melnychuk, S. A.; Liu, C.; Brown, R. S. *Can. J. Chem.* **2009**, *87*, 640. (i) Tsang, W. Y.; Edwards, D. R.; Melnychuk, S. A.; Liu, C. T.; Liu, C.; Neverov, A. A.; Williams, N. H.; Brown, R. S. *J. Am. Chem. Soc.* **2009**, *131*, 4159. (j) Edwards, D. R.; Tsang, W. Y.; Neverov, A. A.; Brown, R. S. *Org. Biomol. Chem.* **2010**, *8*, 822. (k) Brown, R. S.; Lu, Z.-L.; Liu, C. T.; Tsang, W. Y.; Edwards, D. R.; Neverov, A. A. *J. Phys. Org. Chem.* **2010**, *23*, 1. (l) Brown, R. S.; Neverov, A. A. *Adv. Phys. Org. Chem.* **2007**, *42*, 271–331. (m) Brown, R. S. *Prog. Inorg. Chem.* **2011**, *57*, 55–117.

(3) (a) Mancin, F.; Scrimin, P.; Tecilla, P.; Tonellato, U. *Chem. Commun.* **2005**, 2540. (b) Livieri, M.; Mancin, F.; Tonellato, U.; Chin, J. *Chem. Commun.* **2004**, 2862. (c) Mancin, F.; Tecilla, P. *New J. Chem.* **2007**, *31*, 800. (d) Bonomi, R.; Selvestrel, F.; Lombardo, V.; Sissi, C.; Polizzi, S.; Mancin, F.; Tonellato, U.; Scrimin, P. *J. Am. Chem. Soc.* **2008**, *130*, 15744.

(4) (a) Iranzo, O.; Kovalevsky, A. Y.; Morrow, J. R.; Richard, J. P. *J. Am. Chem. Soc.* **2003**, *125*, 1988. (b) Iranzo, O.; Richard, J. P.; Morrow, J. R. *Inorg. Chem.* **2004**, *43*, 1743. (c) Iranzo, O.; Elmer, T.; Richard, J. P.; Morrow, J. R. *Inorg. Chem.* **2003**, *42*, 7737. (d) Yang, M.-Y.; Iranzo, O.; Richard, J. P.; Morrow, J. R. *J. Am. Chem. Soc.* **2005**, *127*, 1064. (e) Yang, M.-Y.; Morrow, J. R.; Richard, J. P. *Bioorg. Chem.* **2007**, *35*, 366. (f) Yang, M.-Y.; Richard, J. P.; Morrow, J. R. *Chem. Commun.* **2003**, 2832. (g) O'Donoghue, A.; Pyun, S. Y.; Yang, M.-Y.; Morrow, J. R.; Richard, J. P. *J. Am. Chem. Soc.* **2006**, *128*, 1615. (h) Morrow, J. R.; Iranzo, O. *Curr. Opin. Chem. Biol.* **2004**, *8*, 192. (i) Nwe, K.; Richard, J. P.; Morrow, J. R. *Dalton Trans.* **2007**, 5171. (j) Farquhar, E.; Richard, J. P.; Morrow, J. R. *Inorg. Chem.* **2007**, *46*, 7169. (k) Mathews, R. A.; Rossiter, C. S.; Morrow, J. R.; Richard, J. P. *Dalton Trans.* **2007**, 3804. (l) Humphry, T.; Iyer, S.; Iranzo, O.; Morrow, J. R.; Richard, J. P.; Panethe, P.; Hengge, A. C. *J. Am. Chem. Soc.* **2008**, *130*, 17858.

(5) (a) Linjalahti, H.; Feng, G.; Mareque-Rivas, J. C.; Mikkola, S.; Williams, N. H. *J. Am. Chem. Soc.* **2008**, *130*, 4232. (b) Feng, G.; Mareque-Rivas, J. C.; Williams, N. H. *Chem. Commun.* **2006**, 1845. (c) Feng, G.; Natale, D.; Prabaharan, R.; Mareque-Rivas, J. C.; Williams, N. H. *Angew. Chem., Int. Ed.* **2006**, *45*, 7056. (d) Feng, G.; Mareque-Rivas, J. C.; de Rossales, R. T. M.; Williams, N. H. *J. Am. Chem. Soc.* **2005**, *127*, 13470. (e) Schroeder, G. K.; Lad, C.; Wyman, P.; Williams, N. H.; Wolfenden, R. *Proc. Natl. Acad. Sci. U.S.A.* **2006**, *103*, 4052. (f) Korhonen, H.; Mikkola, S.; Williams, N. H. *Chem.—Eur. J.* **2012**, *18*, 659.

(6) Gao, H.; Ke, Z.; Deyonker, N. J.; Wang, J.; Xu, H.; Mao, Z.-W.; Phillips, D. L.; Zhao, C. *J. Am. Chem. Soc.* **2011**, *133*, 2904.

(7) Fan, Y.-B.; Gao, Y.-Q. *Acta Phys. Chim. Sin.* **2010**, *26*, 1034.

(8) The k_{cat} values for the cleavages of **2**, **3**, and **4** when bound to **1a** are $(4.1 \pm 0.3) \times 10^{-2}$ s^{-1},[2d] 2300 ± 800 s^{-1},[2a] and 3.10 ± 007 s^{-1},[2a] which amount to a 10^{12}-fold acceleration for all of these substrates relative to their background methoxide-promoted reactions at the pH where the complex was studied.

(9) The k_{cat} value for the **1a**-promoted cyclization of **3** is not an experimental one but is derived from a linear Brønsted regression of a series of substrates for which the rate-limiting step is a chemical one.[2f]

(10) Becke, A. D. *Phys. Rev. A* **1988**, *38*, 3098. (b) Lee, C.; Yang, W.; Parr, R. G. *Phys. Rev. B* **1988**, *37*, 785.

(11) (a) Hay, P. J.; Wadt, W. R. *J. Chem. Phys.* **1985**, *82*, 270. (b) Wadt, W. R.; Hay, P. J. *J. Chem. Phys.* **1985**, *82*, 284.

(12) Tomasi, J.; Mennuccia, B.; Cancés, E. *THEOCHEM* **1999**, *464*, 211. (b) Tomasi, J.; Mennuccia, B.; Cammi, R. *Chem. Rev.* **2005**, *105*, 2999.

(13) Frisch, M. J.; Trucks, G. W.; Schlegel, H. B.; Scuseria, G. E.; Robb, M. A.; Cheeseman, J. R.; Scalmani, G.; Barone, V.; Mennucci, B.; Petersson, G. A.; Nakatsuji, H.; Caricato, M.; Li, X.; Hratchian, H. P.; Izmaylov, A. F.; Bloino, J.; Zheng, G.; Sonnenberg, J. L.; Hada, M.; Ehara, M.; Toyota, K.; Fukuda, R.; Hasegawa, J.; Ishida, M.; Nakajima, T.; Honda, Y.; Kitao, O.; Nakai, H.; Vreven, T.; Montgomery, J. A., Jr.; Peralta, J. E.; Ogliaro, F.; Bearpark, M.; Heyd, J. J.; Brothers, E.; Kudin, K. N.; Staroverov, V. N.; Kobayashi, R.; Normand, J.; Raghavachari, K.; Rendell, A.; Burant, J. C.; Iyengar, S. S.; Tomasi, J.; Cossi, M.; Rega, N.; Millam, N. J.; Klene, M.; Knox, J. E.; Cross, J. B.; Bakken, V.; Adamo, C.; Jaramillo, J.; Gomperts, R.; Stratmann, R. E.; Yazyev, O.; Austin, A. J.; Cammi, R.; Pomelli, C.; Ochterski, J. W.; Martin, R. L.; Morokuma, K.; Zakrzewski, V. G.; Voth, G. A.; Salvador, P.; Dannenberg, J. J.; Dapprich, S.; Daniels, A. D.; Farkas, Ö.; Foresman, J. B.; Ortiz, J. V.; Cioslowski, J.; Fox, D. J. *Gaussian 09*, revision C.01; Gaussian, Inc.: Wallingford, CT, 2009.

(14) Liu, C. T.; Maxwell, C. I.; Edwards, D. R.; Neverov, A. A.; Mosey, N. J.; Brown, R. S. *J. Am. Chem. Soc.* **2010**, *132*, 16599.

(15) (a) Sumimoto, M.; Iwane, N.; Takahama, T.; Sakaki, S. *J. Am. Chem. Soc.* **2004**, *126*, 10457. (b) Tamura, H.; Yamasaki, H.; Sato, H.; Sakaki, S. *J. Am. Chem. Soc.* **2003**, *125*, 16114. (c) Sakaki, S.; Takayama, T.; Sumimoto, M.; Sugimoto, M. *J. Am. Chem. Soc.* **2004**, *126*, 3332.
(16) McNaught, A. D.; Wilkinson, A. *IUPAC Compendium of Chemical Terminology (The "Gold Book")*, 2nd ed; Blackwell Scientific Publications: Oxford, U.K., 1997. Nic, M.; Jirat, J.; Kosata, B.; Jenkins, A. IUPAC Gold Book (corrected XML online version). http://goldbook.iupac.org (accessed Oct 22, 2013).
(17) Binding was not observed for substrate **3**. However, k_{cat} values were determined for a series of aryl-substituted substrates having leaving groups with higher pK_a values than *p*-nitrophenol (ref 2a), and a k_{cat} value for substrate **3** was assigned assuming a linear Brønsted relationship.
(18) For another example of general-base-promoted catalysis of the cyclization of **3** promoted by a Ln(III) ion in 80% DMSO/water, see: Sánchez-Lombardo, I.; Yatsimirsky, A. K. *Inorg. Chem.* **2008**, *47*, 2514.
(19) Mikkola, S.; Stenman, E.; Nurmi, K.; Yousefi-Salakdeh, E.; Strömberg, R.; Lönnberg, H. *J. Chem. Soc., Perkin. Trans. 2* **1999**, 1619.
(20) McCue, K. P.; Morrow, J. R. *Inorg. Chem.* **1999**, *38*, 6136.
(21) (a) Kim, J.; Lim, H. *Bull. Korean Chem. Soc.* **1999**, *20*, 491. (b) An active form cannot be generated in water by following the same general protocol as used to generate the active form in alcohol,[2] namely, by subsequent addition of ligand, 2 equiv of metal ion, and 1 equiv of lyoxide. See: Liu, C. T.; Brown, R. S. Unpublished observations.
(22) (a) Pauling, L. *Nature* **1948**, *161*, 707. (b) Pauling, L. *Am. Sci.* **1948**, *36*, 51.
(23) Zhang, X.; Houk, K. N. *Acc. Chem. Res.* **2005**, *38*, 379.
(24) For an introductory list of literature on the importance or lack of conformational mobility in enzyme-promoted chemical steps of catalysis, see: (a) Závodszky, P.; Kardos, J.; Svingor, Á; Petsko, G. A. *Proc. Natl. Acad. Sci. U.S.A.* **1998**, *95*, 7406. (b) Eisenmesser, E. Z.; Millet, O.; Labeikovsky, W.; Korzhnev, D. M.; Wolf-Watz, M.; Bosco, D. A.; Skalicky, J. J.; Kay, L. E.; Kern, D. *Nature* **2005**, *438*, 117. (c) Banerjee, D.; Pal, S. K. *Langmuir* **2008**, *24*, 8163. (d) Agarwal, P. K. *J. Am. Chem. Soc.* **2005**, *127*, 15248. (e) Hammes-Schiffer, S.; Benkovic, S. J. *Annu. Rev. Biochem.* **2006**, *75*, 519. (f) Agarwal, P. K. *Microb. Cell Fact.* **2006**, *5*, 2. (g) Henzler-Wildman, K. A.; Lei, M.; Thai, V.; Kerns, S. J.; Karplus, M.; Kern, D. *Nature* **2007**, *450*, 913. (h) Bhabha, G.; Lee, J.; Ekiert, D. C.; Gam, J.; Wilson, I. A.; Dyson, H. J.; Benkovic, S. J.; Wright, P. E. *Science* **2011**, *332*, 234. (i) Kamerlin, S. C. L.; Warshel, A. *Proteins* **2010**, *78*, 1339. (j) Kokkinidis, M.; Glykos, N. M.; Fadouloglou, V. V. *Adv. Protein Chem. Struct. Biol.* **2012**, *87*, 182. (k) Gagne, D.; Doucet, N. *FEBS J.* **2013**, DOI: 10.1111/febs.12371. (l) López-Canul, V.; Roca, M.; Bertrán, J.; Moliner, V.; Tuñón, I. *J. Am. Chem. Soc.* **2010**, *132*, 6955.
(25) For reviews, see: (a) Hatanoa, M.; Ishihara, K. *Chem. Commun.* **2012**, *48*, 4273. (b) Jarvo, E. R.; Miller, S. J. *Tetrahedron* **2002**, *58*, 2481. (c) Johnson, R. A.; Sharpless, K. B. In *Catalytic Asymmetric Synthesis*; Ojima, A., Ed.; Wiley: New York, 1993; pp 103−158. (d) Jacobsen, E. N. In *Catalytic Asymmetric Synthesis*; Ojima, A., Ed.; Wiley: New York, 1993; pp 159−202. (e) Tang, W.; Zhang, X. *Chem. Rev.* **2003**, *103*, 3029. (f) Brown, J. M. In *Comprehensive Asymmetric Catalysis*; Jacobsen, E. N., Pfaltz, A., Yamamoto, H., Eds.; Springer: Berlin, 1999; Vol. *1*, Chapter 5.1. (g) Mlynarski, J.; Paradowska, J. *Chem. Soc. Rev.* **2008**, *37*, 1502. (h) Ohkuma, T. *Proc. Jpn. Acad., Ser. B: Phys. Biol. Sci.* **2010**, *86*, 202. (i) Pu, L.; Yu, H.-B. *Chem. Rev.* **2001**, *101*, 757.